

## Article

# Chromatographic Characterization of Archaeological Molluscan Colorants via the Di-Mono Index and Ternary Diagram

Zvi C. Koren 

The Edelstein Center for the Analysis of Ancient Artifacts, Department of Chemical Engineering, Shenkar College of Engineering, Design and Art, 12 Anna Frank St., Ramat Gan 52526, Israel; zvi@shenkar.ac.il

**Abstract:** One of the main research questions regarding archaeological molluscan purple pigments and dyes is whether it is possible to determine which malacological species produced these colorants. For this determination of the zoological provenance of the pigment, a multicomponent analysis must be performed, which can only be obtained from the HPLC technique—the optimal method for identifying all the detectable colorants in a sample. In order to find any trends in the compositions of the dye components from various species of purple-producing sea snails, a statistical formulation is needed. Though principal component analysis (PCA) is a powerful statistical tool that has been used in the analysis of these components, it is based on an algorithm that combines all the componential values and produces new two-dimensional parameters whereby the individualities of the original dye component values are lost. To maintain the integrity of the dye compositions in the purple pigments, a very simple formulation was first published in 2008 and applied to a limited number of samples. This property is known as DMI (short for Di-Mono Index), and for each sample, it is simply the ratio of the peak area of DBI relative to that of MBI, evaluated at the standard wavelength of 288 nm, which has been used for such peak calculations. Currently, considerably more modern and archaeological pigments have been analyzed via HPLC; thus, in the current study, the DMI has been expanded to characterize these purple pigments. Furthermore, a ternary diagram comprising the blue, violet, and red components that can be found in purple colorants is presented for both modern and archaeological purple pigments from the three Muricidae species known in antiquity to produce purple pigments. This triangular diagram is intuitive, retains the integrity of the original dyes, and is presented here for the first time. Both the DMI and the ternary diagram can discern whether a *Hexaplex trunculus* species or perhaps the *Bolinus brandaris* or *Stramonita haemastoma* species were used to produce the pigment. Further, these two representations can also determine whether the IND-rich or the DBI-rich varieties, or both, of *H. trunculus* were used to produce the purple pigment, either as a paint pigment or as a textile dye.

**Keywords:** HPLC; indigoids; indirubinoids; dibromoindigo; molluscan purple pigments and dyes; Muricidae; *Hexaplex trunculus*; Di-Mono Index (DMI); ternary diagram



Citation: Koren, Z.C.

Chromatographic Characterization of Archaeological Molluscan Colorants via the Di-Mono Index and Ternary Diagram. *Heritage* **2023**, *6*, 2186–2201. <https://doi.org/10.3390/heritage6020116>

Academic Editor: Vittoria Guglielmi

Received: 8 December 2022

Revised: 14 February 2023

Accepted: 16 February 2023

Published: 19 February 2023



**Copyright:** © 2023 by the author. Licensee MDPI, Basel, Switzerland. This article is an open access article distributed under the terms and conditions of the Creative Commons Attribution (CC BY) license (<https://creativecommons.org/licenses/by/4.0/>).

## 1. Introduction

### 1.1. Introducing the Sea Snails

Of all the natural organic and inorganic pigments and dyes—from flora, fauna, and mineralia—used by ancient civilizations [1–3], there is no other prized colorant than “purple” (with all its variegated shades) produced from certain molluscan species. This marine-derived imperial colorant was not only heralded as such in antiquity by Greek and Roman writers, e.g., Homer, Aristotle, Vitruvius, and Pliny the Elder, but even historic, not so ancient, poets were awed by this molluscan colorant. In the latter case, this wonderment regarding that colorant is uniquely expressed by the famous English poet Robert Browning in his 1855 poem titled “Popularity”, who refers to this supreme colorant as the “dye of dyes” [4].

It is well-known that in antiquity, there were three related species of mollusks in the Eastern Mediterranean, from which a purple pigment can be produced, and these sea snails are also found today. This Muricidae family—commonly referred to as Murex sea snails—consists of *Hexaplex trunculus* (also known as *Murex trunculus*), *Bolinus brandaris* (= *Murex b.*), and *Stramonita haemastoma* (= *Purpura h.*). The shells of these mollusks are shown in Figure 1. The chemistry associated with the natural biochemical production of the purple pigment and its components has been published in detail [5–7].

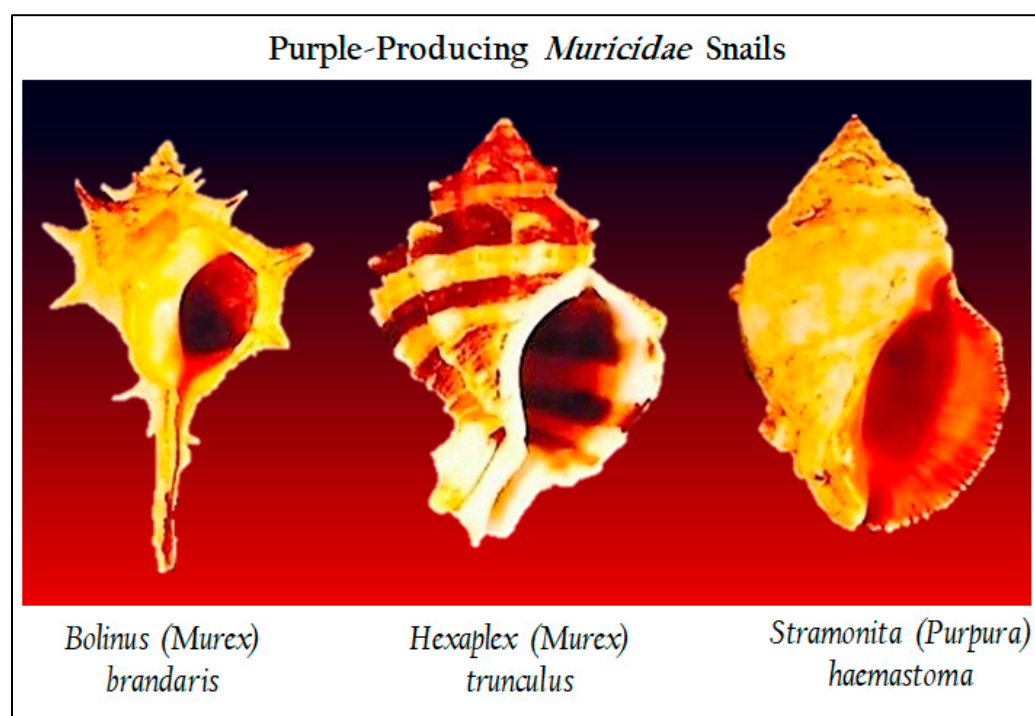


**Figure 1.** Three of the most common purple-producing Mediterranean molluscan species of the *Muricidae* family.

Much has been written about the historical accounts related to these mollusks, and the most prominent ancient historian and science reporter to have written about them was the 1st century CE Roman naturalist Pliny the Elder (Gaius Plinius Secundus). Writing in his monumental multi-volume work *Naturalis Historia*, he recounted the types of sea snails used for purple pigment production, their biology, the season in which to gather them from the seabed, as well as other relevant information. In his role of reporting on the natural world and its animal inhabitants—and keeping in mind that he was obviously not a chemist or alchemist—he nevertheless accurately recounted the entire process of dyeing with these molluscan pigments. Yet, there are modern authors who have at times misunderstood Pliny’s description of the dyeing process. However, if one combines modern chemical principles with his ancient chronicling, it becomes apparent that he correctly described the primary and auxiliary agents—and their processing—that were needed for the reduction and solubilization of the purple pigment [8].

### 1.2. HPLC Über Alles

As for analyzing the purple pigment and identifying all the detectable colorants in it, the optimal method by far is HPLC (high-performance liquid chromatography). The application of the HPLC method for the analyses of molluscan purple pigments was introduced three decades ago by Jan Wouters and André Verhecken, and they successfully separated four-to-five major components of those pigments [9,10]. With that breakthrough, advancements in HPLC analyses have shown that the purple pigment, especially from the *H. trunculus* species, can consist of about 10 colorants [11]. A typical chromatogram, shown

in Figure 2, presents the separation of these components. The dyes constitute the following three chemical groups:

- Indigoids: blue indigo (IND), violet 6-monobromoindigo (MBI), reddish-purple 6,6'-dibromoindigo (DBI);
- Indirubinoids (all reddish-crimson): indirubin (INR), 6-monobromoindirubin (6MBIR), 6'-monobromoindirubin (6'MBIR), 6,6'-dibromoindirubin (DBIR);
- Isatinoids (yellowish): isatin (IS), 6-bromoisatin (6BIS).

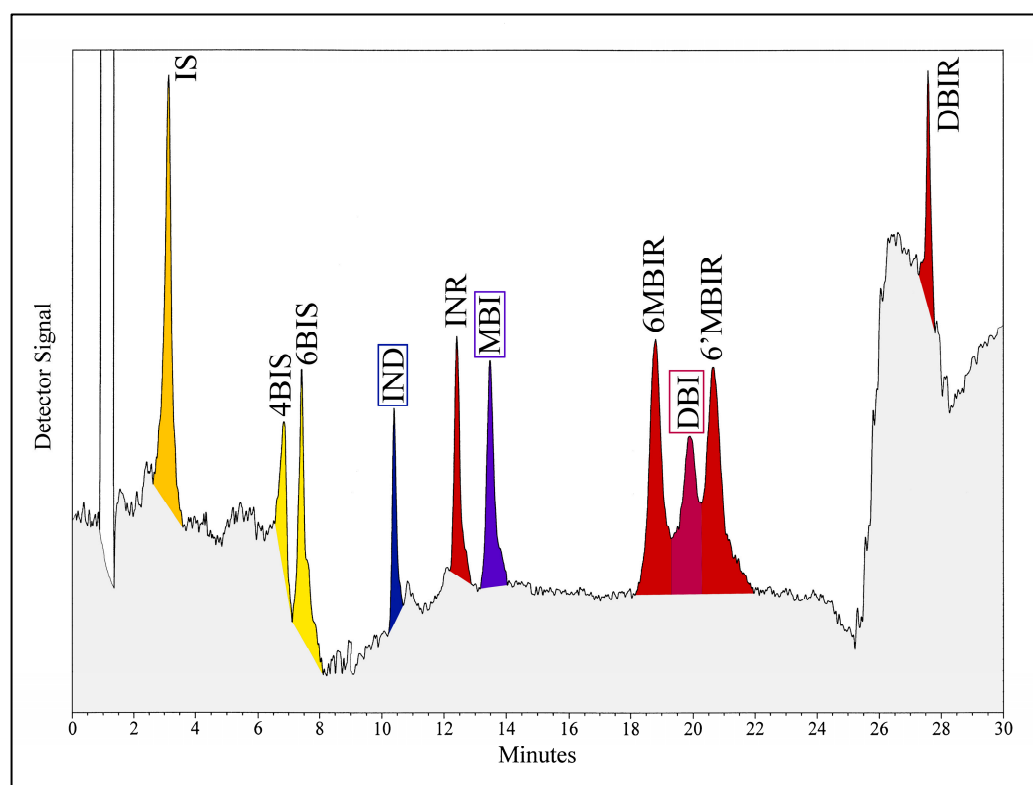


**Figure 2.** HPLC chromatogram of the various indigoids, indirubinoids, and isatinoids (with their representative colors), which may be present in a molluscan purple pigment. Highlighted (in rectangles) are the three main indigoid components present in pigments extracted from *H. trunculus* species.

- The accompanying UV/Vis spectra of these molluscan colorants, as determined by the PDA (photo-diode array) detector of the HPLC, as well as their molecular structures, are shown in Figure 3. The spectra show that each homologous series of dyes has a common visible wavelength at maximum absorption,  $\lambda_{\max}$ , and for the isatinoids, the wavelength is around 415 nm, the indigoids' is about 605 nm, and the indirubinoids' is approximately 540 nm. It is important to note that the  $\lambda_{\max}$  values shown in the UV/Vis absorption spectra are specific for the solvent system in which the dye is solubilized. However, dyes dissolved in other solvents will nevertheless typically yield wavelengths that are close to these values.

Undoubtedly, the most efficient methods for analyzing and identifying relatively non-volatile organic components as whole non-dissociated molecules in a multi-component mixture—such as in the case of the purple pigment—is HPLC. Though GC (gas chromatography) has been used in analyzing molluscan pigments [12], the very high oven temperatures needed for gasifying the components may cause their decomposition, and thus the integrity of the whole molecule may be lost in its identification. Even if only a peripheral fragment has broken away from the parent molecule, this may damage the viability of the analysis itself. For example, the brominated indigoids that constitute the purple pigments from *H. trunculus* are indigo with one bromine atom (MBI) and the doubly

brominated indigo (DBI). In order to obtain an accurate chromatic fingerprinting of these pigments, it is vital that all the original colorant molecules in the pigment remain intact during the analysis. If an analytic method decomposes either DBI or MBI, then artificial amounts of their decomposition products would be formed. If that occurs, then the debromination of MBI would yield an artificial increase in indigo (IND); similarly, if DBI were to decompose during an analysis, then its quantity would be falsely lower. (The quantity of MBI may not change drastically because it would be both formed from DBI and decomposed to IND.) This type of analysis would harm the ability to determine the various colorants in the original sample.

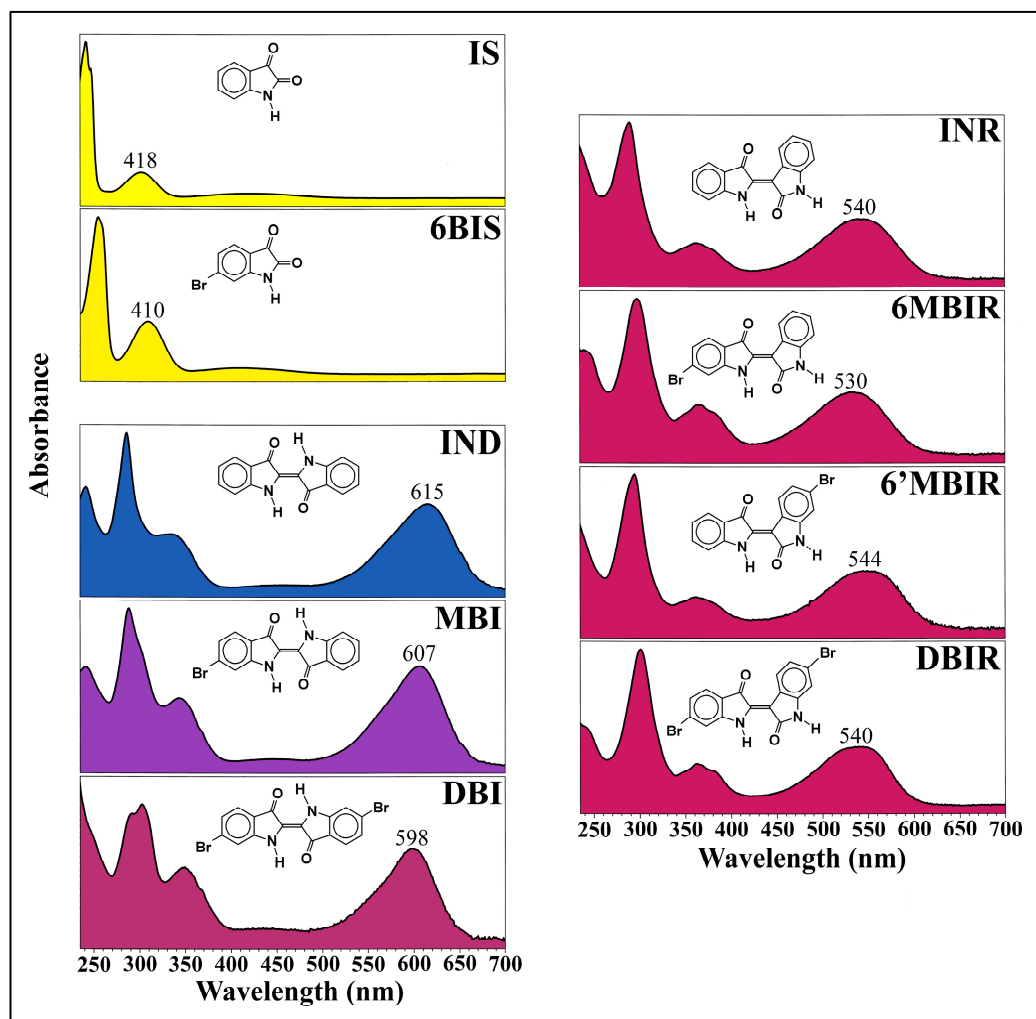


**Figure 3.** UV/Vis spectra and molecular structures of the isatinoids, indigoids, and indirubioids, showing the visible wavelengths at maximum absorption in the methanol/water/ $\text{H}_3\text{PO}_4$  eluent system.

It is important to emphasize the superb detection powers of HPLC to easily “see the invisible” even on the nanogram—or lower—level. Though the HPLC technique is a “destructive” method, it can be described as actually being a “nano-destructive” scheme. As an example of the latter, a successful analysis of a single one- or two-centimeter fiber removed from a yarn of an archaeological textile has been performed via HPLC [13]. This single fiber was effectively invisible to the “naked eye”, but can only be clearly seen via a microscope. With that analysis, a clear separation of four dye components on a single fiber was carried out, with relatively strong HPLC peak signals in the chromatogram.

Analytic methods based on spectrometric techniques have also been used to study dyes, in general, and the purple pigment. These methods include Raman, mass spec-

trometry (MS) without first chromatographically separating the dyes, FTIR, and UV/Vis spectrometry (in the old pioneering days of analysis). However, all of these analytical tools are spectrometric, and the outcome of such an analysis would produce one graph—a spectrum—that is a combination of the spectra of all the components in that pigment. While these techniques may identify the main colorant—or two—in a mixture, spectrometry is limited in that it produces an “overlap of information”. Chromatography yields a “separation of information”, which provides the identification of all the detectable colorants in a pigment or dyeing. This “separation” yields a “chromatic fingerprint” and is essential in trying to identify the biological provenance of the dyestuff, whether from flora or fauna, and from what specific species [14].

### 1.3. Statistical Characterizations of Molluscan Purple

The separating powers of multicomponent HPLC analyses may allow us to determine which malacological species produced the various archaeological pigments and dyes. Towards this end, we need a statistical characterization of the pigments that have been properly analyzed via HPLC. One statistical algorithm for such a characterization is principal component analysis (PCA), and it has been used in the analysis of these components [15,16]. However, this tool has the feeling of a “black box” that incorporates the quantities of the various components, condenses and digests them mathematically, and churns them out in a way that the individuality of the components is lost.

There is a very simple statistical formulation for characterizing molluscan pigments, and it incorporates only two dyes. It was first published in 2008 [17] for a very limited number of samples and has now been expanded to include the results of more recent analyses of archaeological purples. This parameter is known as the Di-Mono Index and is presented in this study to identify the various species of purple-producing mollusks.

Another representation of a statistical characterization of the purple pigments, which maintains the individuality of as many dyes as possible, is the ternary (or triangular) diagram. This graphical depiction best characterizes the dyes so as to allow maximum distinctions among all the species. This intuitive representation would allow for the identification of the zoological provenance of these pigments. This ternary diagram for the molluscan pigments is presented here for the first time.

## 2. Materials and Methods

### 2.1. HPLC: Sample Preparation and Analysis

The sample preparation and the chromatographic elution system used has been previously published [17] and is summarized here. Extraction of the pigment or dye was performed in a glass vial (and not in a plastic one, as the pigment can adhere to the plastic when heated to a high temperature). The duration of the extraction was 5 min via 200–400  $\mu$ L DMSO at 100–150  $^{\circ}$ C, depending on the size of the sample, and in subdued light to prevent the artificial photo-debromination of the components. In order to perform a fully quantitative extraction, no residual color must remain on the sample; thus, additional fresh quantities of DMSO may have been needed for the extraction, and all the extracted solutions were combined.

The resulting hot extracted mixture was immediately filtered in a 0.2- or 0.45- $\mu$  micro-spin polypropylene centrifuge tube with nylon filter for 3 min, and immediately injected into the HPLC. In these analyses, the reverse-phase Waters HPLC system consisted of a 3.0  $\times$  150 mm C<sub>18</sub> symmetry column as the stationary phase, and the ternary eluent system consisted of methanol, water, and 5% H<sub>3</sub>PO<sub>4</sub> as the mobile phase.

### 2.2. Materials Analyzed

The samples analyzed, and their results, consisted of modern and archaeological purple pigments and textile dyes, performed for this study and by other researchers, and are described in Tables 1–3 below in the Results and Discussion section. For the current

study, a number of Roman Period archaeological textiles found in the Judean Desert, Israel, have been analyzed and reported in Table 3.

### 3. Comparison Problems

#### 3.1. Problems in Comparing Results from Different Researchers

In order to build as full a picture as possible regarding the characterization of archaeological molluscan colorants, the analytical results of all laboratories need to be combined. However, there are inherent problems in comparing and integrating results from different researchers. Firstly, for reasons described above, only HPLC results will be considered, as this is the only method through which the multi-components in the sample can be determined. Comparing analytical results from different researchers who used different extraction methods and conditions is risky, and it is important to recognize the potential problems that may be encountered, which are detailed below.

##### 3.1.1. Extraction in Minimal Light

Extraction of the dye or pigment should be performed under subdued lighting conditions so that there is just enough light to see the experimental setup. Performing an extraction in a well-lit laboratory room will, at least partially, photo-debrominate the dissolved colorants; thus, the results of dye analyses will be artificially skewed to less DBI and more IND, as mentioned above regarding the limitations of GC analyses. (The quantity of MBI may change only slightly as it is both formed from the debromination of DBI and decomposed when irradiated.) Analysts have not, in general, designated whether their sample extractions were performed in subdued light and this can be a problem when using their results.

##### 3.1.2. Maximizing Extraction via the Optimal Solvent, Temperature, and Time

Different analysts have used different solvents for extracting the pigments [18]. Firstly, in any system, the solubility of a solute will vary when attempting to dissolve it in different solvents. The components in the purple pigment are no exception. The various solubilities of the purple's components have been studied and published [15]. A further factor in the ability of a solvent to dissolve a sample is the temperature of the mixture and the duration of the extraction process. Thus, these three factors (choice of solvent, temperature, and time) may produce different results for the composition of the colorant when analyzing the same sample, if at least one of these three factors is different among the researchers.

Examples of the effective solvents that have been used for the extraction–dissolution of the indigoids and related compounds in the pigment, and the corresponding temperatures and times, include the following:

- Pyridine: 100 °C [9,10];
- DMF: 150 °C, 3 min [19]; 80 °C, 60 min [20]
- DMSO: 100–150 °C, 5 min [17]; 80 °C, 15–30 min [15]

Though the indigoids have good solubilities in all of these hot solvents, the most effective solvent in dissolving the most stubborn of the indigoids—DBI—is DMSO at high temperatures of 100–150 °C, depending on the quantity of the sample. Even when the extraction is performed in subdued light, as mentioned above, no debromination occurs even at 150 °C as analyzed using HPLC.

It is important to mention that the acidic-methanolic system for extracting mordant dyes is poor in extracting purple's components. What is a good extracting solvent system for mordant dyes is not necessarily effective for vat dyes. In the typical aluminum–dye complex that is formed in naturally dyed textiles, the acid is needed in order to break the metal–dye bond, and the organic solvent (methanol) is then needed for dissolving the dye that was set free. However, the solubilities of the indigoids in that acid–methanol system are very low, where the solubilities decrease from IND to MBI to DBI. Thus, when using that methanol–acid system, the artificial compositions will show relatively high values for IND, lower than actual for MBI, and much lower for DBI. Additionally, if any indirubin

and related brominated derivatives are present, and though their solubilities in methanol are relatively low but higher than the indigoids, then the reported indirubinoid content would also be artificially skewed higher. Thus, the results obtained from the acid–methanol extracting system were not incorporated in the current study.

### 3.1.3. Immediate Filtration and Injection into the HPLC

As soon as the indigoids are extracted into the solvent, the hot mixture should be immediately filtered and injected into the HPLC, so as to preserve the indigoids in the solution. The automation that is found in modern HPLC/UPLC instruments, with the sample tray able to contain tens of sample vials to be tested, should not be employed for analyzing indigoids. Experiments conducted in this laboratory have shown that if, e.g., DBI is dissolved in hot DMSO and left for extended periods of time, then that dye begins to precipitate out of the solution; thus, an analysis of the solution will not produce the correct compositions. Additionally, even in the dark, the indigoids will eventually decompose, at least in part, to yellowish isatinoids. This precipitation phenomenon is probably due to the occurrence of an association between the solute particles as they can form intermolecular hydrogen bonds among themselves and thus produce larger, heavier, molecules—aggregates or agglomerates. These associated complexes and the low room temperature can cause the indigoids to precipitate out of the solution.

### 3.1.4. HPLC Elution Methods

Different stationary and mobile phases, as well as elution methods, have been utilized to chromatographically separate the indigoids in the purple pigment. The nature of the eluents used affects the solubilities of the components in the column's stationary phase. Thus, as the absorption of light of the HPLC detector is measured for each eluting component, different eluents may produce different absorbances as the solutions are different. Even if two researchers use the same mobile phase solvents, but their time-dependent gradient elution methods are different, the compositions of the mobile phases may be different. Thus, using different stationary and mobile phases and different changes of the volumes of the eluents with time may yield different results for the compositions of the purple colorant among the various researchers.

### 3.1.5. HPLC Detection Wavelength

When comparing the results of the HPLC analyses on a set of dyes, the same wavelength of detection of the dye component must be used throughout since different wavelengths will yield different absorptions of light in the UV or visible regions. The wavelength chosen is the one at which all of the investigated dyes have significant light absorptions; thus, these absorptions may be used for comparison purposes. The current standard of absorbance measurements for indigoids is 288 nm, which was first used by Wouters and Verhecken [9,10] and has been adopted by others. If the measured ability of each component to absorb light at a given wavelength is known—and this is known as absorptivity ( $a$ ) or extinction coefficient ( $\epsilon$ )—then the actual mass of each dye component can be ascertained. However, not all of the researchers of this purple pigment have used the same wavelength in their measurements; thus, initially, these values cannot be used for comparing one set of measurements at one wavelength with another set of results at a different wavelength. However, this apparent problem may be overcome by knowing the ratio of absorbances at the different wavelengths and then re-calculating the absorbance at the desired wavelength.

When measuring the absorbance of each indigoid, it may be best not to first measure its absorbance at the UV wavelength of choice (288 nm), but rather at the visible wavelength at which the dye in question has its maximum absorbance,  $\lambda_{\max}$ . Afterwards, knowing the ratio of absorbances at the standard UV wavelength and the visible wavelength, a calculation of the absorbance at 288 nm can be performed. This type of re-calculation was previously performed [17] and was also conducted in the current study. The reasoning for measuring at the visible wavelength first is that an archaeological sample has impurities

from the ground in which it was excavated, and some of these non-colorants may absorb UV light at or approximately the standard UV wavelength. Thus, directly measuring the peak area at the time of the eluting dye at the standard UV wavelength, may partially mask its actual peak, thereby reducing its peak purity and possibly incorporating into it the absorbance of not only the dye, but also of the impurities, which would produce a false measurement.

## 4. Results and Discussion

### 4.1. Modern and Archaeological Purples

Considering all of the limitations and concerns about combining the analytical HPLC results from various analysts, as discussed above, it is, nevertheless, expected that all the analytical results would not deviate far from their true values in order to obtain an overall pattern for the dye components. The results of different researchers were also incorporated into the PCA studies mentioned above.

The following tables show the integrated peak area values as percentages for the five main indigoid and indirubinoid components that can be found in modern and archaeological pigments produced from the purple-producing sea snails. These data are all based on an effective extraction system and the HPLC methodology discussed above. A form of these tables was initially determined by Karapanagiotis et al. [15,16,21] and has now been expanded in the current work to include more samples and information.

The following sample descriptions appear in the tables below: the geographical region where the pigment or dye was produced; a description of the manner in which the colorant was obtained; the solvent used for sample preparation as well as the temperature and heating duration; the HPLC-produced integrated peak areas (as %) of the five main components evaluated at 288 nm; and the original literature reference that discusses these samples in detail. For completeness purposes, each colorant's DMI value, which is discussed below, is also shown in the tables.

Table 1 outlines the information regarding purple pigments produced from modern *H. trunculus* sea snails from different researchers, and each sample was given a "T" number in the tables that were previously established, as mentioned above [15,16,21]. Similarly, Table 2 shows the relevant data regarding modern *B. brandaris* and *S. haemastoma* pigments, and these samples are given "B" and "H" numbers, respectively.

Table 3 lists the various archaeological materials—pigments and textile dyes—that have been analyzed. These historic items span parts of the globe from the Aegean Sea to the Mediterranean and the Middle East to Siberia and England, and are dated from the 17th century BCE up to about only a century ago.

**Table 1.** Relative dye components (calculated at 288 nm as % peak areas via the HPLC-PDA detector) of modern *Hexaplex trunculus* colorants.

Sample	Region	Description	Solvent Temp., Time *	IND	Dye Components				DMI **	Reference
					INR	MBI	DBI	DBIR		
T1	Carthage, Tunisia	Shells crushed and exposed to air and sunlight	DMSO 80, 15	62.90	1.20	32.10	3.70	0.10	0.12	[15]
T2	Croatia	Snails removed from water, exuding pigment when expiring	DMSO 80, 15	49.80	4.40	37.60	7.10	1.10	0.19	[15]
T3	Tunisia	Tunisia “red”; gland excised in the dark	DMSO 80, 15	35.10	0.40	49.70	14.40	0.40	0.29	[15]
T4	Tunisia	Tunisia “blue”: T3 pigment in boiling water	DMSO 80, 15	54.00	1.50	39.40	4.90	0.20	0.12	[15]
T5	Tarragona, Spain	Stained, non-vatted, cotton	Pyridine 100, ?	56.00	0.00	37.00	7.00	0.00	0.19	[9,10]
T6	Tarragona, Spain	Vat-dyed wool	Pyridine 100, ?	53.00	14.00	33.00	0.00	0.00	0.00	[9,10]
T7	Akhziv, Israel	Pigment extracted from glands at the seashore	DMF 100, 5	4.05	0.00	17.79	60.00	18.16	3.37	[17,22]
T8	Saronikos, Greece	Glands exposed to 6 h sunlight, extracting 1 h with DMF, and dried	DMF 80, 15	35.20	8.10	30.50	15.80	10.40	0.52	[15,20]
T9	Akhziv, Israel	Same as T7	DMSO 100, 5	0.35	0.00	7.41	68.39	23.85	9.23	[17]
T10	Spain	Pigment	DMSO 100, 5	40.72	3.34	41.33	4.25	10.36	0.10	[17]
T11	France	Pigment on talc substrate	DMSO room, 10	10.30	2.90	44.40	36.80	5.60	0.83	[23]
T12	Hermione, Greece	Pigment	DMF ?, ?	27.80	7.50	37.40	23.20	4.10	0.62	[15]
T13	Thessaloniki, Greece	Excised glands exposed to direct sunlight for 3 h	DMSO 80, 30	7.3	2.2	30.4	22.9	37.2	0.75	[21]

\* A question mark appears if the temperature and /or duration of heating were not reported in the publication. \*\* A blue color for the DMI value is indicative of an IND-rich *H. trunculus* pigment, and a red color represents a DBI-rich *H. trunculus* pigment; see text for the detailed discussions.

**Table 2.** Relative dye components (calculated at 288 nm as % peak areas via the HPLC-PDA detector) of modern *Bolinus brandaris* and *Stramonita haemastoma* colorants.

Sample	Region	Description	Solvent Temp., Time	IND	Dye Components				DMI	Reference
					INR	MBI	DBI	DBIR		
<i>Bolinus brandaris</i>										
B1	Tarragona, Spain	Sample was stained cotton (not vat)	Pyridine 100, ?	0.00	0.00	0.00	85.00	15.00	∞	[9,10]
B2	Tarragona, Spain	Sample was dyed wool (vat)	Pyridine 100, ?	0.00	0.00	6.00	81.00	13.00	13.5	[9,10]
B3	Saronikos, Greece	Glands exposed to 6 h sunlight, extracting 1 h with DMF, and dried	DMF 80, 15	0.001	0.00	1.60	97.20	1.20	60.8	[15,20]
B4	Fiumicino, Italy	Pigment	DMSO 100, 5	0.00	0.00	1.36	94.88	3.76	69.8	[17]
B5	Thera, Greece	Glands exposed to direct sunlight for 3 h	DMSO 80, 30	2.00	0.50	1.80	79.30	16.40	44.1	[21,24]
<i>Stramonita haemastoma</i>										
H1	Tarragona, Spain	Stained, not vatted, cotton	Pyridine 100, ?	0.00	0.00	3.00	91.00	6.00	30.3	[9,10]
H2	Tarragona, Spain	Dyed, vatted, wool	Pyridine 100, ?	0.00	0.00	3.00	91.00	6.00	30.3	[9,10]
H3	Palmahim, Israel	Pigment extracted at seashore	DMSO 100, 5	0.00	0.00	0.86	85.48	13.66	99.4	[17]

**Table 3.** Relative dye components (calculated at 288 nm as % peak areas via the HPLC-PDA detector) of archaeological colorants. All extractions performed in DMSO.

Sample	Region	Description	Period	IND	Dye Components				DMI	Reference
					INR	MBI	DBI	DBIR		
Ak1 *	Akrotiri	Lump of purple pigment		1.10	0.00	20.10	71.80	7.00	<b>3.57</b>	[15]
Ak2 *	Akrotiri	Purple pigment from wall painting	17th c. BCE	1.70	0.00	18.80	77.60	1.90	<b>4.13</b>	[15]
Ak3 *	Akrotiri	Purple pigment in New Pillar Pit		3.20	0.00	27.10	65.90	3.80	<b>2.43</b>	[15]
Tr *	Trianda	Purple pigment		2.50	0.00	24.40	66.20	6.90	<b>2.71</b>	[15]
Ra *	Raos	Purple pigment from wall painting		1.60	0.00	15.50	77.30	5.60	<b>4.99</b>	[15]
E1 *	Greece	Epitaphios textile, Benaki Museum	Byzantine14th c. CE	48.60	0.00	25.90	25.00	0.50	<b>0.97</b>	[15]
E2 *	Greece	Painted decoration on burial couch		48.00	0.40	25.40	25.60	0.60	<b>1.01</b>	[15]
DsP *	Daskyleion, Turkey	Textile from the burial site	5th c. BCE	21.3	0.1	31.4	8.8	38.4	<b>0.28</b>	[21]
DsT *		Purple fabric from sarcophagus		14.0	0.1	42.0	12.8	31.1	<b>0.30</b>	[21]
Ro *	Thessaloniki	Pigment from painted stone jar	3rd c. CE	2.50	0.00	32.70	58.30	6.50	<b>1.78</b>	[16]
Da **	Iran	Polychrome textile in Katoen Natie, Antwerp	5th c. BCE	0.19	0.00	14.84	82.61	2.36	<b>5.57</b>	[17]
K1 ***	Egypt			50.50	0.00	35.10	13.70	0.70	<b>0.39</b>	[13]
K2 ***	Egypt		5th c. CE	28.98	0.00	42.48	26.88	1.66	<b>0.63</b>	[13]
K3 ***	Egypt			2.36	0.00	53.48	43.02	1.14	<b>0.80</b>	[13]
J1 **			1st c. BCE	11.23	0.08	36.05	50.62	2.02	<b>1.40</b>	Herein
J2 **				33.07	0.07	48.15	17.89	0.82	<b>0.37</b>	Herein
J3 **				22.01	0.34	28.19	49.47	0.00	<b>1.76</b>	Herein
J4 **			1st c. BCE—1st c. CE	19.35	0.25	45.53	34.87	0.00	<b>0.77</b>	Herein
J5 **	Judean Desert, Israel	Various purple textiles from Ancient Israel		11.76	0.00	40.28	47.97	0.00	<b>1.19</b>	Herein
J6 **				34.19	0.00	30.68	33.84	1.29	<b>1.10</b>	Herein
J7 **				3.87	2.54	46.61	46.99	0.00	<b>1.01</b>	Herein
J8 **				89.00	0.00	10.00	1.00	0.00	<b>0.10</b>	Herein
J9 **			2nd c. CE	90.40	0.00	9.10	0.50	0.00	<b>0.05</b>	Herein
J10 **				56.16	0.00	35.56	8.28	0.00	<b>0.23</b>	Herein
P0 **	Siberia			6.7	0.00	44.6	48.6	0.00	<b>1.09</b>	Herein
P1 **	Siberia	Pazyryk polychromic saddle cloth	4th c. BCE	26.1	0.00	56.4	17.5	0.00	<b>0.31</b>	Herein
P2 **	Siberia			30.9	0.00	51.49	17.6	0.00	<b>0.34</b>	Herein
P3 **	Siberia			15.9	0.00	44.9	39.2	0.00	<b>0.87</b>	Herein
L **	Leeds, UK	Purple-dyed cotton of C.S. Bedford	≥1910 CE	12.00	0.00	1.00	87.00	0.00	<b>87.00</b>	[25]

\* DMSO extraction at 80 °C for 15 min. \*\* DMSO extraction at 100 °C, 5 min. \*\*\* DMSO extraction at 150 °C, 5 min.

#### 4.2. Di-Mono Index

In order to classify all the malacological pigments, and based on that categorization, be able to determine the zoological provenance of the purple pigment, a simple predictive index was developed. This indicator is known as the Di-Mono Index (DMI), and for each sample, it is the ratio of the peak area of DBI relative to that of MBI, measured at the standard 288 nm wavelength:

$$DMI = A(DBI)/A(MBI) @ 288 \text{ nm}$$

The reason that IND, which is found in *H. trunculus* pigments, was not chosen for this property is because one cannot rule out the fact that the indigo may not have solely originated from a molluscan source but that a plant-based indigo was added. It is especially important to emphasize that there have been dyeings that were found to be double-dyed with a molluscan source and either madder, a red-scale insect, and, perhaps, even plant indigo.

In the three tables, the DMI values are also presented. From the values of Table 1, it could be discerned that there is a difference among *H. trunculus* snails, and that some pigments have very low DMI values and others have higher numbers. On the other hand, Table 2 shows that the non-*H. trunculus* snails have very high values.

Figure 4 shows the DMI values for modern pigments produced from *H. trunculus* obtained from different geographical regions (listed in Table 1). It is apparent that for *H. trunculus* snails, the IND-rich (i.e., DBI-poor) bluish or violet pigments have a DMI of up to about 0.6, whereas the DBI-rich reddish pigments have DMI values from about 0.8 to 9.

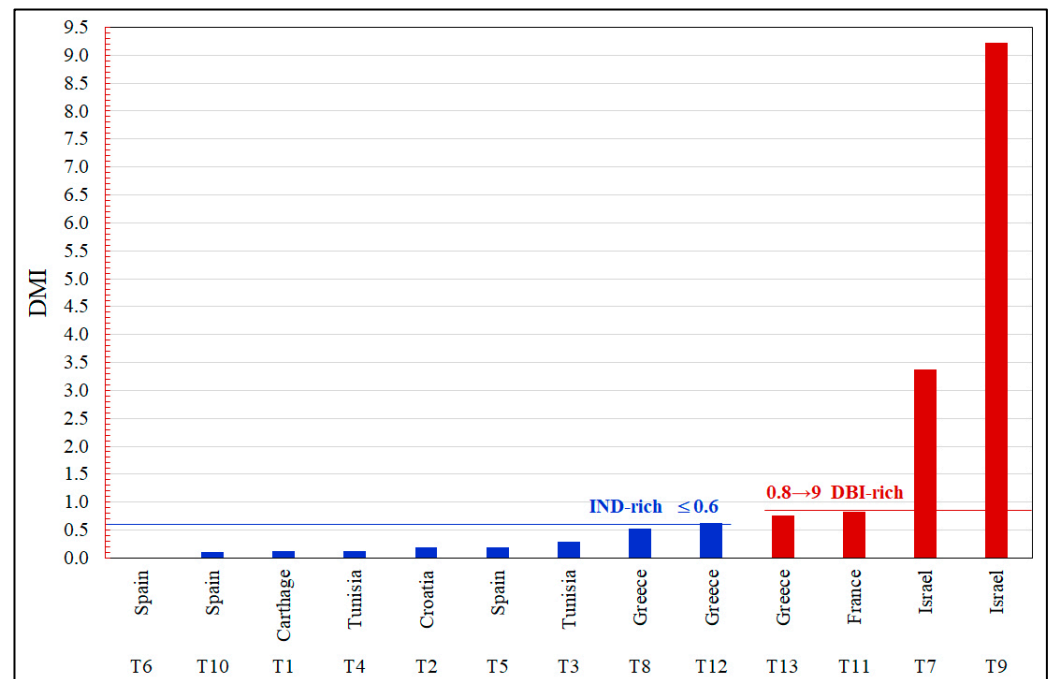


Figure 4. DMI values for modern *H. trunculus* from different geographical regions.

The DMI values for purple pigments from the non-*trunculus* Mediterranean snails—*B. brandaris* and *S. haemastoma*—are shown in Figure 5.

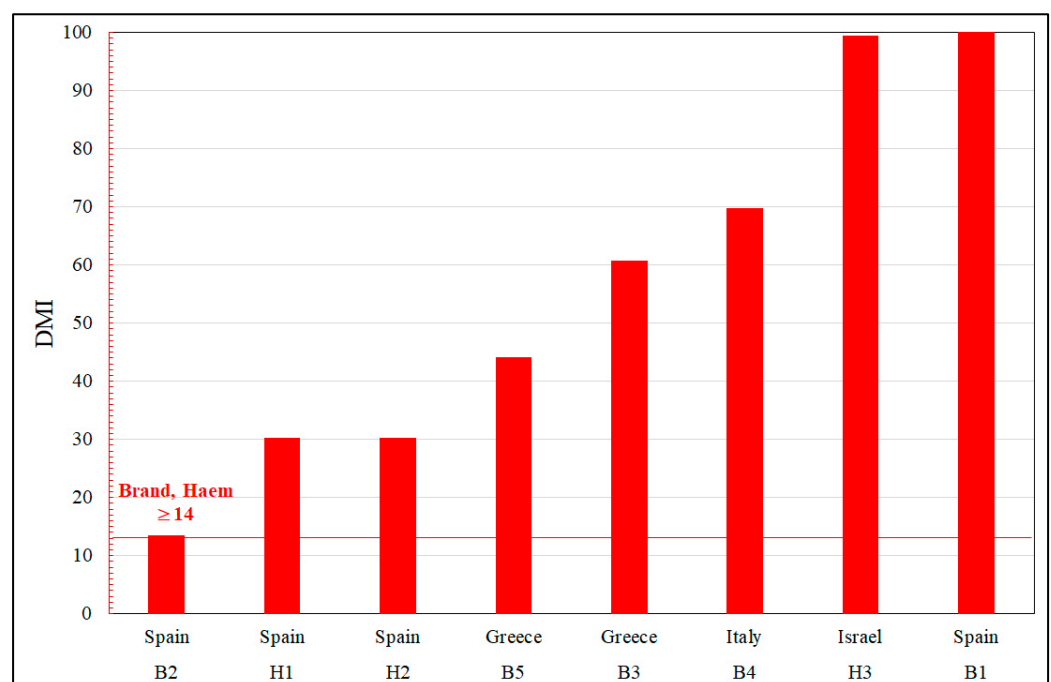


Figure 5. DMI values for modern *B. brandaris* (B) and *S. haemastoma* (H) from different geographical regions.

The DMI values shown in Figure 5 are very high, significantly higher than even the DBI-rich *H. trunculus* snails. However, as the *B. brandaris* and *S. haemastoma* share these very high DMI values, it is not possible to differentiate between the pigments from these two species. These elevated values can be simply explained by the special nature of the MBI component, whose properties have been studied [26]. The very high DMI values for non-*trunculus* snail pigments are due to their very low and even negligible quantities of MBI in their pigments, whereas, in general, all *trunculus*-based pigments—whether reddish- or bluish-purple—have significant amounts of MBI [27]. From Figure 5 and Table 2, it is observed that when using the optimal extracting solvent (DMSO) for these analyses, the pigments from non-*trunculus* snails have DMI values greater than 40, which is nearly five times the highest value for the DBI-rich *trunculus* pigment with the highest DMI value.

Except for one special case of a historic century-old dyeing from Leeds (UK), which was dyed with non-*trunculus* snails off the African coast [25], all the archaeological samples reported in Table 3 have DMI values of less than 6. This is indicative of *H. trunculus* pigments as depicted in Figure 4. Thus, based on the DMI property alone, it could be inferred that the archaeological samples were produced from *H. trunculus* snails that are either IND-rich (with  $DMI < 0.6$ ) or DBI-rich (DMI between 0.8–9). It is, of course, possible that both types of *H. trunculus* were mixed, or even that some non-*trunculus* snails were used as red-color additives. However, most probably, the *H. trunculus* was always used.

#### 4.3. Ternary Diagram

The ternary diagram (also known as a triangular diagram) incorporating the results of the HPLC analyses on modern and archaeological samples is depicted in Figure 6.

The ternary diagram is an aesthetic visual method of presenting multicomponent data in a graphical manner. Ternary or triangular diagrams were first used in the mid-18th century [28] and have become a standard method of data display today for samples that contain at least three components or condensed into three. Numerous examples are found of the use of ternary diagrams in many areas of science related to archaeological or modern samples in, e.g., metallurgy and geology [29–31], physical chemistry and material science [32–34], and botany and zoology [35–37].

Though it is represented in two-dimensional space, the ternary diagram maintains the identities of all the main original dyes and their colors, blue (IND), violet (MBI), and reds.

In the triangular chart, each apex represents 100% of the corresponding dye, and the opposite base designates 0%. In the diagram, IND and MBI are denoted as such, and the third coordinate, labelled “reds”, includes the sum of all the main dye components that yield reddish colors, specifically, DBI, DBIR, and INR. Thus, the apex at the top represents 100% IND, the apex at the bottom left designates 100% MBI, and the apex at the bottom right represents 100% “reds”. All the various colors from the five main components that could be present in molluscan purple pigments are represented in this diagram, which maintains the individual original identities of the dyes.

The ternary diagram shows that the IND-rich *H. trunculus* pigments are clustered in the middle-to-upper left of the chart within a semi-oval (also known mathematically as a semi-stadium). This positioning is as expected for these indigo-rich and DBI-poor pigments. The chart also indicates that the DMI values for this semi-oval group is  $\leq 0.6$ , as discussed in the tables above. The other variety, the DBI-rich *H. trunculus* species, are grouped at the bottom right within a shoe-shape arrangement, with DMI values ranging from 0.8–9. The other Muricidae sea snails, *B. brandaris* and *S. haemastoma*, are compressed to occupy a miniscule area at the extreme bottom right, as expected, for these pigments that are even more red than the DBI-rich *H. trunculus* species. Their DMI values, as also previously noted, are  $\geq 14$ , and the optimal DMSO extractions  $> 40$ .

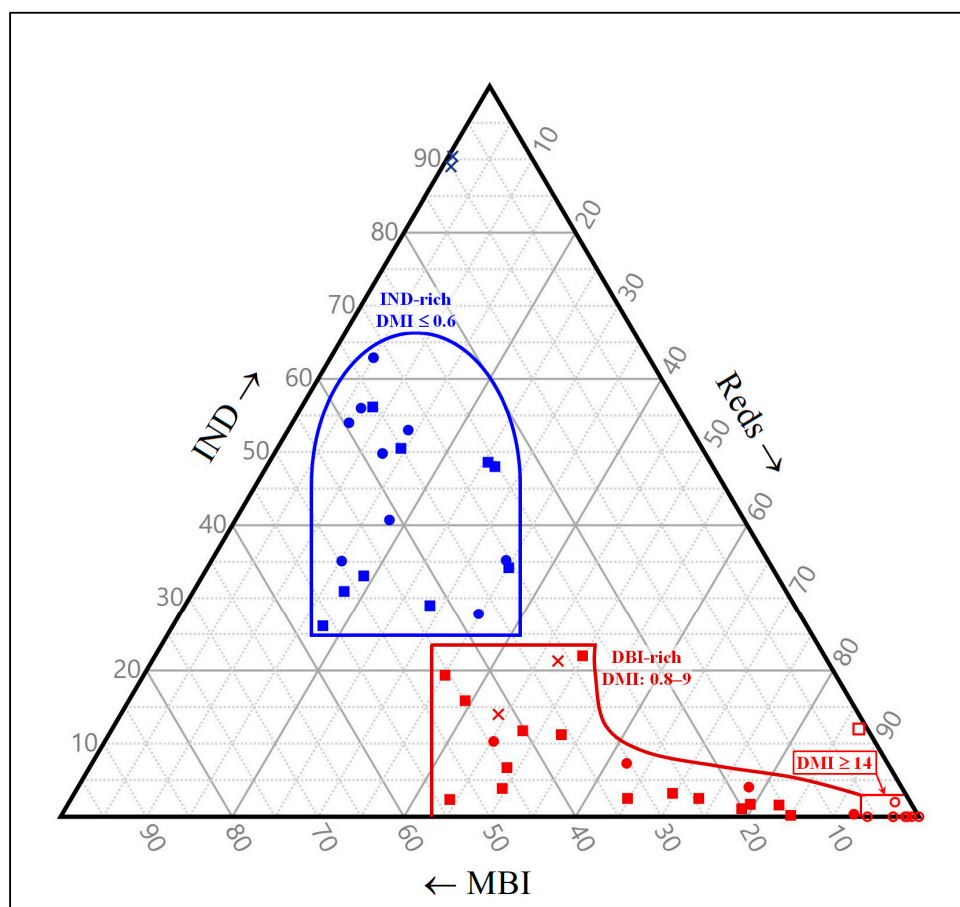


**Figure 6.** Ternary diagram showing the relative dye compositions (as % peak areas in the HPLC chromatogram at 288 nm) of pigments produced from modern and archaeological Muricidae sea snail species. The “reds” axis and apex represent the sum of all the main reddish components (DBI, DBIR, INR). The open red circles at the extreme bottom right represent modern *B. brandaris* and *S. haemastoma* purples; the closed circles represent modern *H. trunculus* pigments (blue for IND-rich and red for DBI-rich pigments). The squares and Xs represent various archaeological samples.

The ternary diagram shown in Figure 6 also includes the various archaeological purple pigments and dyes. With very few exceptions, all the archaeological colorants appear within the semi-oval or shoe-shaped areas, and no archaeological pigment is present in the small shape to the right of the tip of the “shoe”, which is inhabited by the *B. brandaris* and *S. haemastoma* pigments. This indicates that all archaeological molluscan purples were probably produced from *H. trunculus* species, either the IND-rich or DBI-rich varieties. The red-only non-*H. trunculus* snails may have been added to the DBI-rich *H. trunculus* pigments to produce even redder dyeings. It is important to mention that the archaeological pigments represented by the points present at the borders between the semi-oval and the shoe shape could have been produced from a combination of the two varieties of *H. trunculus* snails.

It is important to note how the two statistical formulations presented in this paper complement each other to determine the zoological provenance of a molluscan pigment. For example, at the tip of the “shoe” in the ternary diagram lies pigment T9 (a DBI-rich *trunculus*), which borders B2 (*brandaris*); thus, it seems that they are nearly clustered together. However, their DMI values are significantly different: the *trunculus* pigment’s DMI value is about 9 and the *brandaris* is 14.

## 5. Conclusions

The presence of any brominated dye in a colorant automatically indicates that the source of this pigment or dye is malacological, since only sea snails can produce that kind

of colorant. HPLC analyses of various modern and archaeological molluscan pigments have shown that *H. trunculus* snails are unique, different from all other purple-producing snails from all of the world's waters. The pigments from all purple-producing sea snails contain DBI—this is the common dye of all molluscan purple pigments. However, all non-*H. trunculus* mollusks produce mainly DBI; thus, their purple pigments are always reddish. The singularity of *H. trunculus* is that its pigments contain all three indigoids (as well as indirubinoids): DBI (as all do), MBI, and IND. This major point about the exclusivity of *H. trunculus* snails is that they alone contain a significant amount of MBI, which is what distinctly separates them from all other species, and is observed in their DMI values.

Further, it was found that within the *H. trunculus* species, there are two varieties—maybe even subspecies—where one type produces reddish-purple pigments and another produces bluish-purple (violet) pigments. The *H. trunculus* snails producing reddish-purple pigments are DBI-rich, more than IND; however, these pigments are not as reddish as the pigments from non-*H. trunculus* snails, which mostly have DBI in their pigment. The other variety of *H. trunculus* produces bluish-purple or violet pigments because of the overwhelming amount of IND in the pigment, and they are IND-rich. Both types of pigments are termed the generic “purple”, which is not a pure color but a mixture of red and blue. A schematic summary of the differences among the sea snails is depicted in Figure 7. While the *H. trunculus* has probably always been used in Mediterranean pigments, the other snails were also employed, not alone but as color additives, if desired, to produce even redder dyeings than those obtained from the DBI-rich *H. trunculus*.

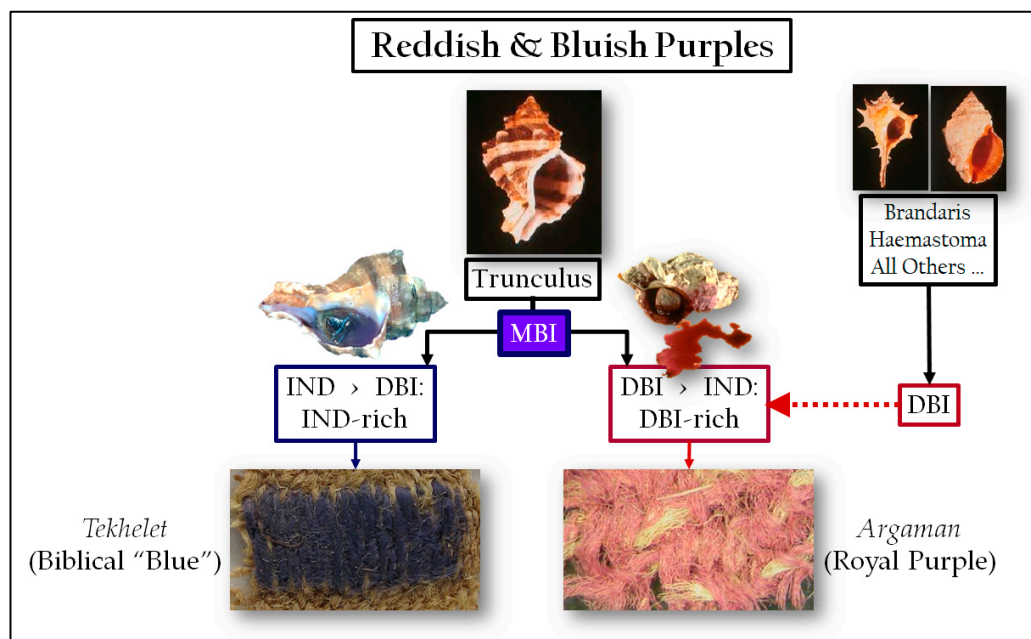


**Figure 7.** Relative compositions of reddish-purple and bluish-purple pigments produced from *H. trunculus*, and reddish-purple pigments from all other mollusks. In addition, a Roman Period Royal Purple textile (the biblical *Argaman* color) from King Herod (1st c. BCE) and 1st c. BCE—1st c. CE violet, bluish-purple yarns (dyed to the biblical *Tekhelet* color) are also shown, both excavated at Masada in the Judean Desert, Israel.

The uniqueness of the current research is that to date, the characterization of the three color components (reddish, violet, and bluish) of molluscan purple pigments by means of a ternary diagram has not been applied. This is one of the major innovative themes of the study. This type of classification should therefore become an accepted standard for characterizing the various color components of such molluscan colorants in order to enable quantitative comparisons among them by using a more visual—and aesthetic—statistical formulation for these samples. The current study has shown that by combining the DMI

values with the ternary diagram, the malacological identities of molluscan purple pigments can be determined.

**Funding:** This research received no external funding.

**Acknowledgments:** The author is most grateful for the support given to the research on natural dyes by the Sidney and Mildred Edelstein Foundation.

**Conflicts of Interest:** The author declares no conflict of interest.

## References

1. Cardon, D. *Natural Dyes: Sources, Tradition, Technology and Science*; Archetype Publications: London, UK, 2007.
2. Orna, M.V. *March of the Pigments: Color History, Science and Impact*; Royal Society of Chemistry: London, UK, 2022.
3. Orna, M.V. *The Chemical History of Color*; Springer Briefs in Molecular Science, History of Chemistry, Springer Science & Business Media: Heidelberg, Germany; New York NY, USA, 2012; Chapter 4; pp. 47–78.
4. Koren, Z.C. Archaeological shades of purple from flora and fauna from the ancient Near East. In *Archaeological Chemistry: A Multidisciplinary Analysis of the Past*; Orna, M.V., Rasmussen, S., Eds.; Cambridge Scholars Publishing: Newcastle upon Tyne, UK, 2020; Chapter 13; pp. 256–300.
5. Cooksey, C.J. Tyrian Purple: 6,6'-dibromoindigo and related compounds. *Molecules* **2001**, *6*, 736–769. [[CrossRef](#)]
6. Cooksey, C. Tyrian purple: The first four thousand years. *Sci. Prog.* **2013**, *96*, 171–186. [[CrossRef](#)]
7. Karapanagiotis, I. A Review on the Archaeological Chemistry of Shellfish Purple, Special Issue “Natural Sciences in Archaeology and Cultural Heritage”. *Sustainability* **2019**, *11*, 3595. [[CrossRef](#)]
8. Koren, Z.C. New chemical insights into the ancient molluscan purple dyeing process. In *Archaeological Chemistry VIII*; ACS Symposium Series 1147; Armitage, R.A., Burton, J.H., Eds.; American Chemical Society: Washington, DC, USA, 2013; Chapter 3; pp. 43–67.
9. Wouters, J.; Verhecken, A. High-performance liquid chromatography of blue and purple indigoid natural dyes. *J. Soc. Dye. Colour.* **1991**, *107*, 266–269. [[CrossRef](#)]
10. Wouters, J. A new method for the analysis of blue and purple dyes in textiles. *Dye. Hist. Archaeol.* **1992**, *10*, 17–21.
11. Koren, Z.C. HPLC-PDA analysis of brominated indirubinoid, indigoid, and isatinoid dyes. In *Indirubin, the Red Shade of Indigo*; Meijer, L., Guyard, N., Skaltsounis, L., Eisenbrand, G., Eds.; Life in Progress Editions: Roscoff, France, 2006; Chapter 5; pp. 45–53.
12. Koh, A.; Apostolakou, V.; Pareja, M.N.; Crandall, A.M.; Betancourt, P.P. Organic residue studies. In *Alatzomouri Pefka: A Middle Minoan IIB Workshop Making Organic Dyes*; Apostolakou, V., Brogan, T.M., Betancourt, P.P., Eds.; INSTAP Academic Press: Philadelphia, PA, USA, 2020; Chapter 13; pp. 111–118.
13. Koren, Z.C.; Verhecken-Lammens, C. Microscopic and chromatographic analyses of molluscan purple yarns in a late Roman Period textile. *E-Preserv. Sci.* **2013**, *10*, 27–34.
14. Koren, Z.C. Editorial: Extracting thousands of years of colorful dye history through analytical science. *Palest. Explor. Q.* **2011**, *143*, 1–3. [[CrossRef](#)]
15. Karapanagiotis, I.; Mantzouris, D.; Cooksey, C.; Mubarak, M.S.; Tsiamyrtzis, P. An improved HPLC method coupled to PCA for the identification of Tyrian Purple in archaeological and historical samples. *Microchem. J.* **2013**, *110*, 70–80. [[CrossRef](#)]
16. Karapanagiotis, I.; Sotiropoulou, S.; Vasileiadou, S.; Karagiannidou, E.; Mantzouris, D.; Tsiamyrtzis, P. Shellfish purple and gold threads from a Late Antique tomb excavated in Thessaloniki. *Arachne* **2018**, *5*, 64–77.
17. Koren, Z.C. Archaeo-chemical analysis of Royal Purple on a Darius I stone jar. *Microchim. Acta* **2008**, *162*, 381–392. [[CrossRef](#)]
18. Degano, I.; Ribechini, E.; Modugno, F.; Colombini, M.P. Analytical methods for the characterization of organic dyes in artworks and in historical textiles. *Appl. Spectrosc. Rev.* **2009**, *44*, 363–410. [[CrossRef](#)]
19. Koren, Z.C. Methods of dye analysis used at the Shenkar College Edelstein Center in Israel. *Dye. Hist. Archaeol.* **1993**, *11*, 25–33.
20. Karapanagiotis, I.; de Villemereuil, V.; Magiatis, P.; Polychronopoulos, P.; Vougianniopoulou, K.; Skaltsounis, A.-L. Identification of the coloring constituents of four natural indigoid dyes. *J. Liq. Chromatogr. Relat. Technol.* **2006**, *29*, 1491–1502. [[CrossRef](#)]
21. Papiaka, Z.E.; Konstanta, A.; Karapanagiotis, I.; Karadag, R.; Akyol, A.A.; Mantzouris, D.; Tsiamyrtzis, P. FTIR imaging and HPLC reveal ancient painting and dyeing techniques of molluscan purple. *Archaeol. Anthropol. Sci.* **2017**, *9*, 197–208. [[CrossRef](#)]
22. Koren, Z.C. High-performance liquid chromatographic analysis of an ancient Tyrian Purple dyeing vat from Israel. *Isr. J. Chem.* **1995**, *35*, 117–124. [[CrossRef](#)]
23. Nowik, W.; Marciniowska, R.; Kusiak, K.; Cardon, D.; Trojanowicz, M. High performance liquid chromatography of slightly soluble brominated indigoids from Tyrian Purple. *J. Chromatogr. A* **2011**, *1218*, 1244–1252. [[CrossRef](#)] [[PubMed](#)]
24. Mantzouris, D.; Karapanagiotis, I. Identification of indirubin and monobromoindirubins in *Murex brandaris*. *Dye. Pigment.* **2014**, *104*, 194–196. [[CrossRef](#)]
25. Whitworth, I.; Koren, Z.C. Orchil and Tyrian Purple: Two centuries of Bedfords from Leeds. *Ambix* **2016**, *63*, 244–267. [[CrossRef](#)]
26. Clark, R.J.H.; Cooksey, C.J. Monobromoindigos: A new general synthesis, the characterization of all four isomers and an investigation into the purple colour of 6,6'-dibromoindigo. *New J. Chem.* **1999**, *23*, 323–328. [[CrossRef](#)]
27. Koren, Z.C. Monobromoindigo: The singular chromatic biomarker for the identification of the malacological provenance of archaeological purple pigments from *Hexaplex trunculus* species. In *Ancient Textile Production from an Interdisciplinary Perspective*:

- Humanities and Natural Sciences Interwoven for our Understanding of Textiles; Interdisciplinary Contributions to Archaeology*; Ulanowska, A., Grömer, K., Vanden Berghe, I., Öhrman, M., Eds.; Springer: Cham, Switzerland, 2022; Chapter 3; pp. 39–52.
28. Howarth, R.J. Sources for a history of the ternary diagram. *Br. J. Hist. Sci.* **1996**, *29*, 337–356. [[CrossRef](#)]
  29. Chirikure, S. Geochemistry of ancient metallurgy: Examples from Africa and elsewhere. In *Treatise on Geochemistry*, 2nd ed.; Turekian, K.K., Holland, H.D., Eds.; Elsevier: Amsterdam, The Netherlands, 2014; Chapter 14.13; pp. 169–189.
  30. Hsu, Y.-K.; Sabatini, B.J. A geochemical characterization of lead ores in China: An isotope database for provenancing archaeological materials. *PLoS ONE* **2019**, *14*, e0215973. [[CrossRef](#)]
  31. Morel, M.; Serneels, V. Interpreting the Chemical Variability of Iron Smelting Slag: A Case Study from Northeastern Madagascar. *Minerals* **2021**, *11*, 900. [[CrossRef](#)]
  32. Cardell, C.; Guerra, I.; Sánchez-Navas, A. SEM-EDX at the Service of Archaeology to Unravel Historical Technology. *Microsc. Today* **2009**, *17*, 28–33. [[CrossRef](#)]
  33. Chiarella, R.A.; Davey, R.J.; Peterson, M.L. Making co-crystals—The utility of ternary phase diagrams. *Cryst. Growth Des.* **2007**, *7*, 1223–1226. [[CrossRef](#)]
  34. Dhoot, A.S.; Naha, A.; Priya, J.; Xalxo, N. Phase diagrams for three component mixtures in pharmaceuticals and its applications. *J. Young Pharm.* **2018**, *10*, 132–137. [[CrossRef](#)]
  35. Gholizadeh, F.; Mirzaghaderi, G. Genome-wide analysis of the polyamine oxidase gene family in wheat (*Triticum aestivum* L.) reveals involvement in temperature stress response. *PLoS ONE* **2020**, *15*, e0236226. [[CrossRef](#)]
  36. Yang, L.; Danzberger, J.; Schöler, A.; Schröder, P.; Schloter, M.; Radl, V. Dominant groups of potentially active bacteria shared by barley seeds become less abundant in root associated microbiome. *Front. Plant Sci.* **2017**, *8*, 1005. [[CrossRef](#)] [[PubMed](#)]
  37. Discamps, E.; Costamagno, S. Improving mortality profile analysis in zooarchaeology: A revised zoning for ternary diagrams. *J. Archaeol. Sci.* **2015**, *58*, 62–76. [[CrossRef](#)]

**Disclaimer/Publisher’s Note:** The statements, opinions and data contained in all publications are solely those of the individual author(s) and contributor(s) and not of MDPI and/or the editor(s). MDPI and/or the editor(s) disclaim responsibility for any injury to people or property resulting from any ideas, methods, instructions or products referred to in the content.